UT-HET-092
KU-PH-014

Radiative neutrino mass, dark matter and electroweak baryogenesis from the supersymmetric gauge theory with confinement

Shinya Kanemura[a], Naoki Machida[a], Tetsuo Shindou[b]

[a] *Department of Physics, University of Toyama, 3190 Gofuku, Toyama, 930-8555, Japan*
[b] *Division of Liberal-Arts, Kogakuin University, 1-24-2 Nishi-Shinjuku, Tokyo, 163-8677, Japan*

arXiv:1405.5834v1 [hep-ph] 22 May 2014

Abstract

We propose a simple model to explain neutrino mass, dark matter and baryogenesis based on the extended Higgs sector which appears in the low-energy effective theory of a supersymmetric gauge theory with confinement. We here consider the $SU(2)_H$ gauge symmetry with three flavours of fundamental representations which are charged under the standard $SU(3)_C \times SU(2)_L \times U(1)_Y$ symmetry and a new discrete Z_2 symmetry. We also introduce Z_2-odd right-handed neutrino superfields in addition to the standard model matter superfields. The low-energy effective theory below the confinement scale contains the Higgs sector with fifteen composite superfields, some of which are Z_2-odd. When the confinement scale is of the order of ten TeV, electroweak phase transition can be sufficiently of first order, which is required for successful electroweak baryogenesis. The lightest Z_2-odd particle can be a new candidate for dark matter, in addition to the lightest R-parity odd particle. Neutrino masses and mixings can be explained by the quantum effects of Z_2-odd fields via the one-loop and three-loop diagrams. We find a benchmark scenario of the model, where all the constraints from the current neutrino, dark matter, lepton flavour violation and LHC data are satisfied. Predictions of the model are shortly discussed.

1. Introduction

The Higgs boson has been discovered at the LHC, and its measured properties are currently consistent with the standard model (SM)[1]. However, the minimal Higgs sector in the SM is just an assumption. We still do not know the essence of the Higgs boson and the structure of the Higgs sector. Is the Higgs boson really a scalar particle or otherwise a composite state? What is the fundamental physics behind the Higgs dynamics? What is the origin of vacuum condensation? How many Higgs fields are there? Answers for these

questions directly correspond to the paradigm of the fundamental theory beyond the SM. At the same time, the possibility of various extended Higgs sectors provides us an idea that the Higgs sector would be strongly related to the phenomena such as tiny neutrino masses and mixing[2], the existence of dark matter (DM) [3] and the baryon asymmetry of the Universe (BAU)[3], none of which can be explained in the SM.

Among several possibilities for baryogenesis[4, 5], there is a scenario so-called electroweak baryogenesis[5], where the BAU could be explained by the dynamics of the Higgs potential when the electroweak phase transition is of strongly first order. It is well-known that the electroweak baryogenesis cannot be realized within the SM. Hence, a non-minimal Higgs sector has to be introduced for the successful scenario of electroweak baryogenesis[6–8]. With the discovered Higgs boson mass to be 126 GeV, the condition of the strong first-order phase transition (1stOPT) requires at least one of the self-coupling constants in the Higgs potential to be relatively large. A phenomenological consequence of the theory with the strong 1stOPT is a significantly larger triple Higgs boson coupling than the SM prediction, by which the scenario of the electroweak baryogenesis can be tested at future collider experiments[9]. At the same time, such a large self-coupling constant in the Higgs potential tends to cause early brow-up of the running coupling constant, and the Landau pole[10] can appear at the scale much below the Planck scale[11]. In this case, the ultraviolet picture above the Landau pole should also be considered[12].

One possible explanation for tiny neutrino masses is based on the seesaw mechanism, where neutrino masses are explained at the tree level with introducing very heavy right-handed (RH) neutrinos[13], Higgs triplet fields[14] or fermion triplet fields[15]. An alternative idea is to generate tiny neutrino masses radiatively by introducing extended Higgs sectors at the TeV scale. Since the original model was proposed by A. Zee[16], many models[17–22] have been proposed along this line. In a class of models where neutrino masses are generated radiatively at loop levels, an unbroken discrete Z_2 symmetry and RH neutrinos are introduced such that the RH neutrinos have the odd quantum number to make neutrino Yukawa coupling constants absent at the tree level[17–19, 22]. The same symmetry also guarantees the stability of the lightest Z_2-odd particle, so that it can be a DM candidate. The model proposed by E. Ma (the Ma model) is the simplest model of this category[17] where the neutrino masses are generated at the one-loop level, and in the model proposed in Ref. [18, 19] (the AKS model) they are generated at the three-loop level. Both models have DM candidates. Furthermore, in the AKS model, the strong 1stOPT is also realized. Although these models are phenomenologically acceptable, additional scalar particles are introduced in an *ad-hoc* way which seems rather artificial. Fundamental theories are desirable in which these phenomenological models are deduced in the low-energy effective theory.

In this Letter, we propose a simple model whose low-energy effective theory can explain neutrino mass, DM and baryogenesis. In this model, the supersymmetric (SUSY) extended Higgs sector appears in the low-energy effective theory of a SUSY gauge theory with confinement[23]. With an additional Z_2 symmetry, all the scalar fields introduced in the Ma model and the AKS model automatically appear, so that introducing a RH neutrino superfield with the odd quantum number, neutrino mass, DM and baryogenesis can be

Table 1: The SM charges and the Z_2 parity assignment on the $\mathrm{SU}(2)_H$ doublets T_i and the $\mathrm{SU}(2)_H$ singlet RH neutrino N_R^c.

Superfield	$\mathrm{SU}(2)_H$	$\mathrm{SU}(3)_C$	$\mathrm{SU}(2)_L$	$\mathrm{U}(1)_Y$	Z_2
$\begin{pmatrix} T_1 \\ T_2 \end{pmatrix}$	2	1	2	0	+1
T_3	2	1	1	+1/2	+1
T_4	2	1	1	−1/2	+1
T_5	2	1	1	+1/2	−1
T_6	2	1	1	−1/2	−1
N_R^c	1	1	1	0	−1

explained simultaneously by a hybrid mechanism of the Ma model and the AKS model in the framework of SUSY. Consequently there are two kinds of the DM candidates: *i.e.*, one comes from the lightest R-parity odd SUSY particle, and the other is the lightest Z_2-odd particle, so that the DM scenario of our model is multi-component DM scenario.

We introduce the $\mathrm{SU}(2)_H$ gauge symmetry with three flavours of fundamental representations [12, 24], which are charged under the standard $\mathrm{SU}(3)_C\times$ $\mathrm{SU}(2)_L\times\mathrm{U}(1)_Y$ symmetry and a new discrete Z_2 symmetry. In addition to the SM matter superfields, we also introduce Z_2-odd RH neutrino superfields. Then the low-energy effective theory below the confinement scale contains the Higgs sector with fifteen composite superfields, some of which are Z_2-odd. Electroweak phase transition can be of sufficiently strong first-order, when the confinement scale is of the order of ten TeV [11, 25]. In addition to the lightest R-parity odd particle, the lightest Z_2-odd particle can be a new candidate for DM. We can explain neutrino masses and mixings by the quantum effects of Z_2-odd fields via the one-loop and three-loop diagrams.

We find a benchmark scenario of the model, where all the constraints from the current neutrino[2], DM[3, 26, 27], lepton flavour violation (LFV) [28] and LHC data are satisfied. We also comment on predictions of the model.

2. The SUSY gauge theory with confinement and its low-energy effective theory

Our model is based on a SUSY model with the $\mathrm{SU}(2)_H \times Z_2$ symmetry. We introduce six chiral superfields, T_i $(i = 1, \cdots, 6)$, which are doublet under the $\mathrm{SU}(2)_H$ gauge symmetry. The chiral superfields T_i's also have gauge quantum number under the SM gauge symmetry, $\mathrm{SU}(3)_C \times \mathrm{SU}(2)_L \times \mathrm{U}(1)_Y$, and moreover quantum numbers of the Z_2 parity are assigned. In addition, a RH neutrino superfield N_R^c is also introduced. As similar to the setup proposed in Ref. [25], this is a singlet chiral superfield for both the $\mathrm{SU}(2)_H$ and the SM gauge symmetry but it has an odd parity under the Z_2 symmetry. The SM charges and the Z_2 parity assignments on T_i's and N_R^c are shown in Table 1.

As investigated in Ref. [23], in the SUSY $\mathrm{SU}(2)_H$ gauge theory with three flavours (six doublet chiral superfields), the $\mathrm{SU}(2)_H$ gauge coupling becomes strong at a confinement scale

Table 2: The field contents of the Higgs sector below the confinement scale Λ_H.

Superfield	$SU(3)_C$	$SU(2)_L$	$U(1)_Y$	Z_2
$H_d \equiv \begin{pmatrix} H_{14} \\ H_{24} \end{pmatrix}$	1	2	$-1/2$	$+1$
$H_u \equiv \begin{pmatrix} H_{13} \\ H_{23} \end{pmatrix}$	1	2	$+1/2$	$+1$
$\Phi_d \equiv \begin{pmatrix} H_{15} \\ H_{25} \end{pmatrix}$	1	2	$-1/2$	-1
$\Phi_u \equiv \begin{pmatrix} H_{16} \\ H_{26} \end{pmatrix}$	1	2	$+1/2$	-1
$\Omega_- \equiv H_{46}$	1	1	-1	-1
$\Omega_+ \equiv H_{35}$	1	1	$+1$	-1
$N \equiv H_{56}, N_\Phi \equiv H_{34}, N_\Omega = H_{12}$	1	1	0	$+1$
$\zeta \equiv H_{36}, \eta \equiv H_{45}$	1	1	0	-1

which is denoted by Λ_H, and below Λ_H the low-energy effective theory is described in terms of fifteen canonically normalized mesonic composite chiral superfields, $H_{ij} \simeq \frac{1}{4\pi\Lambda_H} T_i T_j (i \neq j)$ by using the Naive Dimensional Analysis[29]. The fifteen superfields are summarised in Table 2. With these mesonic fields, the superpotential in the Higgs sector of the low-energy effective theory is written as

$$\begin{aligned} W_{\text{eff}} =& \lambda N \left(H_u H_d + v_0^2 \right) + \lambda N_\Phi \left(\Phi_u \Phi_d + v_\Phi^2 \right) + \lambda N_\Omega \left(\Omega_+ \Omega_- - \zeta\eta + v_\Omega^2 \right) \\ & + \lambda \left\{ \zeta H_d \Phi_u + \eta H_u \Phi_d - \Omega_+ H_d \Phi_d - \Omega_- H_u \Phi_u - N N_\Phi N_\Omega \right\} , \end{aligned} \tag{1}$$

where the Naive Dimensional Analysis suggests $\lambda \simeq 4\pi$ at the confinement scale Λ_H. The

relevant soft SUSY breaking terms are given by

$$\begin{aligned}
\mathcal{L}_H =& - m_{H_u}^2 H_u^\dagger H_u - m_{H_d}^2 H_d^\dagger H_d - m_{\Phi_u}^2 \Phi_u^\dagger \Phi_u - m_{\Phi_d}^2 \Phi_d^\dagger \Phi_d \\
& - m_N^2 N^* N - m_{N_\Phi}^2 N_\Phi^* N_\Phi - m_{N_\Omega}^2 N_\Omega^* N_\Omega \\
& - m_{\Omega_+}^2 \Omega_+^* \Omega_+ - m_{\Omega_-}^2 \Omega_-^* \Omega_- - m_\zeta^2 \zeta^* \zeta - m_\eta^2 \eta^* \eta \\
& - \left\{ C\lambda v_0^2 N + C_\Phi \lambda v_\Phi^2 N_\Phi + C_\Omega \lambda v_\Omega^2 N_\Omega + \text{h.c.} \right\} \\
& - \left\{ B\mu H_u H_d + B_\Phi \mu_\Phi \Phi_u \Phi_d + B_\Omega \mu_\Omega (\Omega_+ \Omega_- + \zeta\eta) + \text{h.c.} \right\} \\
& - \lambda \Big\{ A_N H_u H_d N + A_{N_\Phi} \Phi_u \Phi_d N_\Phi + A_{N_\Omega} (\Omega_+ \Omega_- - \eta\zeta) N_\Omega + A_\zeta H_d \Phi_u \zeta \\
& \quad + A_\eta H_u \Phi_d \eta + A_{\Omega_-} H_u \Phi_u \Omega_- + A_{\Omega_+} H_d \Phi_d \Omega_+ + \text{h.c.} \Big\} \\
& - \left\{ m_{\zeta\eta}^2 \eta^* \zeta + \frac{B_\zeta^2}{2} \zeta^2 + \frac{B_\eta^2}{2} \eta^2 + \text{h.c.} \right\} , \qquad (2)
\end{aligned}$$

where the mass parameters $\mu = \lambda\langle N \rangle$, $\mu_\Phi = \lambda\langle N_\Phi \rangle$ and $\mu_\Omega = \lambda\langle N_\Omega \rangle$ are induced after the Z_2-even neutral fields N, N_Φ and N_Ω get vacuum expectation values (vev's). As for the field degrees of freedom of the superfields N_Φ and N_Ω, they are not relevant to the phenomena discussed in this Letter, therefore we ignore them in the following discussion. The tree-level Lagrangian for the Z_2-even Higgs sector is identical to the one in the nearly-minimal SUSY SM (nMSSM)[30].

The matter sector except for the terms relevant to the RH neutrino is almost the same as the one in the minimal SUSY SM (MSSM) or the nMSSM, where we assume that the R-parity is not broken. On the other hand, the relevant superpotential terms to the RH neutrino below the confinement scale Λ_H are given by

$$W_N = y_N^i N_R^c L_i \Phi_u + h_N^i N_R^c E_i^c \Omega_- + \frac{M_R}{2} N_R^c N_R^c + \frac{\kappa}{2} N N_R^c N_R^c , \qquad (3)$$

where L_i and E_i^c denote the lepton doublets and the charged lepton singlets, respectively.

3. Mechanisms for baryogenesis (1stOPT), the neutrino masses and the DM

In the following, we give a brief review on the mechanisms which are adopted in this model for the strong 1stOPT, the neutrino mass generation and the DM.

The condition of the strong 1stOPT, $\varphi_c/T_c \gtrsim 1$, is required for a successful electroweak baryogenesis scenario. As discussed in Refs. [8, 11, 18, 19], non-decoupling effects of the Z_2-odd scalar boson loop can enhance the value of φ_c/T_c. In our model, this mechanism is adopted. In order to realize $\varphi_c/T_c > 1$, the coupling constant between the SM-like Higgs boson h and the Z_2-odd scalars should be large as $\lambda \simeq 1.8$[11], and masses of the relevant Z_2-odd scalars are mainly determined by the contribution from the Higgs vev. For such a large coupling constant as $\lambda \simeq 1.8$, the Landau pole appears at around 5 TeV which will be identified to the confinement scale Λ_H. Above this scale, the theory becomes the SUSY $\mathrm{SU}(2)_H \times Z_2$ gauge theory.

It is known that the same non-decoupling scalar loop effect can also give a significant contribution to the triple Higgs boson coupling λ_{hhh}[9]. If a charged Z_2-odd boson loop gives

a significant contribution to φ_c/T_c, it also affects the process of $h \to \gamma\gamma$. The HL-LHC with the luminosity of 3000fb^{-1} is expected to measure the deviation of B($h \to \gamma\gamma$) from the SM prediction, if it is larger than 10%[31]. The ILC with $\sqrt{s} = 1$ TeV with 2.5 ab^{-1} can test the scenario by measuring the Higgs triple coupling if it deviates in the positive direction from the SM prediction as large as 13%[32].

The neutrino masses in our model are radiatively induced via the hybrid contribution of the one-loop and the three-loop diagrams shown in Fig. 1. The one-loop diagram and the three-loop diagrams are driven by the coupling constants y_N^i and h_N^i, respectively, which are independent with each other. The three-loop contributions are not necessarily suppressed as compared to the one-loop contributions, and both the one-loop and the three-loop diagrams can significantly contribute to generating the neutrino masses. The mass matrix for the neutrino is evaluated as

$$(m_\nu)_{ij} = m_{ij}^{(\mathrm{I})} + m_{ij}^{(\mathrm{II})} \ , \tag{4}$$

where $m_{ij}^{(\mathrm{I})}$ and $m_{ij}^{(\mathrm{II})}$ denote the one-loop and the three-loop contributions, respectively. They can be calculated as

$$m_{ij}^{(\mathrm{I})} = \frac{y_N^i y_N^j}{(4\pi)^2} \left\{ (O_0)^{1\alpha}(O_0)^{1\alpha} m_{\nu_R} - (O_0)^{5\alpha}(O_0)^{5\alpha} m_{\nu_R} \right\} \bar{B}_0(m^2_{\Phi_\alpha}, m^2_{\nu_R}) \ , \tag{5}$$

and

$$\begin{aligned} m_{ij}^{(\mathrm{II})} =& \frac{\hat{\lambda}^4 v_u^2 y_E^i h_N^{i*} y_E^j h_N^{j*} m_{\nu_R}}{(16\pi^2)^3} \\ & \times \sin^4\beta (U_+^*)_{4\gamma}(U_+)_{4\gamma}(U_+^*)_{4\delta}(U_+)_{4\delta} \left\{ (O_0)_{2\rho}(O_0)_{2\rho} - (O_0)_{6\rho}(O_0)_{6\rho} \right\} \\ & \times F(m^2_{\nu_R}, m^2_{\Phi_\rho}; m^2_{e_i}, m^2_{H^\pm}, m^2_{\Phi_\gamma^\pm}; m^2_{e_j}, m^2_{H^\pm}, m^2_{\Phi_\delta^\pm}) \\ & + \frac{2\hat{\lambda}^2 y_E^i h_N^{i*} y_E^j h_N^{j*} m_{\nu_R} m_{\tilde{\Phi}_\gamma^\pm} m_{\tilde{\Phi}_\delta^\pm}}{(16\pi^2)^3} \\ & \times (V_L^*)_{2\alpha}(V_L)_{2\alpha}(V_L^*)_{2\beta}(V_L)_{2\beta}(U_L^*)_{2\gamma}(U_R)_{2\gamma}(U_L^*)_{2\delta}(U_R)_{2\delta} \\ & \times \left\{ (O_0)_{3\rho}(O_0)_{3\rho} - (O_0)_{7\rho}(O_0)_{7\rho} \right\} F(m^2_{\nu_R}, m^2_{\Phi_\rho}; m^2_{\tilde{\chi}_\alpha^\pm}, m^2_{\tilde{e}_{Ri}}, m^2_{\tilde{\Phi}_\gamma^\pm}; m^2_{\tilde{\chi}_\beta^\pm}, m^2_{\tilde{e}_{Rj}}, m^2_{\tilde{\Phi}_\delta^\pm}) \ . \end{aligned} \tag{6}$$

In the above expressions, the mixing matrices O_0, U_+, U_L, U_R and V_L are defined as

$$\begin{pmatrix} \Phi_u^{\rm even} \\ \zeta^{\rm even} \\ \Phi_d^{\rm even} \\ \eta^{\rm even} \\ \Phi_u^{\rm odd} \\ \zeta^{\rm odd} \\ \Phi_d^{\rm odd} \\ \eta^{\rm odd} \end{pmatrix} = O_0 \begin{pmatrix} \Phi_1 \\ \Phi_2 \\ \Phi_3 \\ \Phi_4 \\ \Phi_5 \\ \Phi_6 \\ \Phi_7 \\ \Phi_8 \end{pmatrix} , \quad \begin{pmatrix} \Phi_u^+ \\ \Omega_+ \\ (\Phi_d^-)^* \\ (\Omega_-)^* \end{pmatrix} = U_+ \begin{pmatrix} \Phi_1^+ \\ \Phi_2^+ \\ \Phi_3^+ \\ \Phi_4^+ \end{pmatrix} ,$$

$$\begin{pmatrix} \tilde{\Phi}_d^- \\ \tilde{\Omega}_- \end{pmatrix} = U_L \begin{pmatrix} \tilde{\Phi}_{1L}^- \\ \tilde{\Phi}_{2L}^- \end{pmatrix} , \quad \begin{pmatrix} (\tilde{\Phi}_u^+)^* \\ (\tilde{\Omega}_+)^* \end{pmatrix} = U_R \begin{pmatrix} \tilde{\Phi}_{1R}^- \\ \tilde{\Phi}_{2R}^- \end{pmatrix} , \quad \begin{pmatrix} \tilde{W} \\ \tilde{H}_d^- \end{pmatrix} = V_L \begin{pmatrix} \tilde{\chi}_{1L}^- \\ \tilde{\chi}_{2L}^- \end{pmatrix} , \tag{7}$$

where the superscript "even" and "odd" denote the CP-even neutral scalar component and CP-odd neutral scalar component, the scalar fields Φ_i are the mass eigenstates of Z_2-odd neutral scalars, the scalar fields $\Phi_i^\pm$ are the mass eigenstates of Z_2-odd charged scalars, the fermionic fields $\tilde{\Phi}_{iL}^-$ and $\tilde{\Phi}_{iR}^-$ are the left-handed and the right-handed components of the mass eigenstates of the Z_2-odd charged fermions, $\tilde{W}$ denotes the wino in the SUSY SM, and $\tilde{\chi}_{iL}^-$ are the left-handed component of the mass eigenstates of the Z_2-even charginos. The loop function $\bar{B}_0$ is given by

$$\bar{B}_0(m_1^2, m_2^2) = -\frac{m_1^2 \ln m_1^2 - m_2^2 \ln m_2^2}{m_1^2 - m_2^2} , \tag{8}$$

and the loop function F is given by[18, 19]

$$\begin{aligned} & F(M^2, m_\Phi^2; m_{\chi 1}^2; m_{\phi 1}^2, m_{\Omega 1}^2; m_{\chi 2}^2; m_{\phi 2}^2, m_{\Omega 2}^2) \\ & = \frac{(16\pi^2)^3}{i} \int \frac{d^D k}{(2\pi)^D} \frac{1}{k^2 - M^2} \frac{1}{k^2 - m_\Phi^2} \int \frac{d^D p}{(2\pi)^D} \frac{\not{p}}{p^2 - m_{\chi 1}^2} \frac{1}{p^2 - m_{\phi 1}^2} \frac{1}{(k+p_1)^2 - m_{\Omega 1}^2} \\ & \quad \times \int \frac{d^D q}{(2\pi)^D} \frac{(-\not{q})}{(-q)^2 - m_{\chi 2}^2} \frac{1}{(-q)^2 - m_{\phi 2}^2} \frac{1}{(k+(-q))^2 - m_{\Omega 2}^2} . \end{aligned} \tag{9}$$

Due to the difference in the flavour structure between $m_{ij}^{(\rm I)}$ and $m_{ij}^{(\rm II)}$, two finite mass eigenvalues of light neutrinos are induced, even though only one RH neutrino are introduced.

The flavour structure in the RH neutrino sector significantly contributes to the LFV processes such as $\mu \to e\gamma$ and $\mu \to eee$, which give strong constraint on the model parameter space. The contributions to the $\mu \to e\gamma$ process are from the diagram shown in Fig. 2-(a). The branching ratio B($\mu \to eee$) is suppressed by factor $\frac{\alpha}{4\pi}$ as compared to the branching ratio B($\mu \to e\gamma$), unless the box contribution shown in Fig. 2-(b) dominates the branching ratio B($\mu \to eee$). If the box contribution is significant, the $\mu \to eee$ process gives an

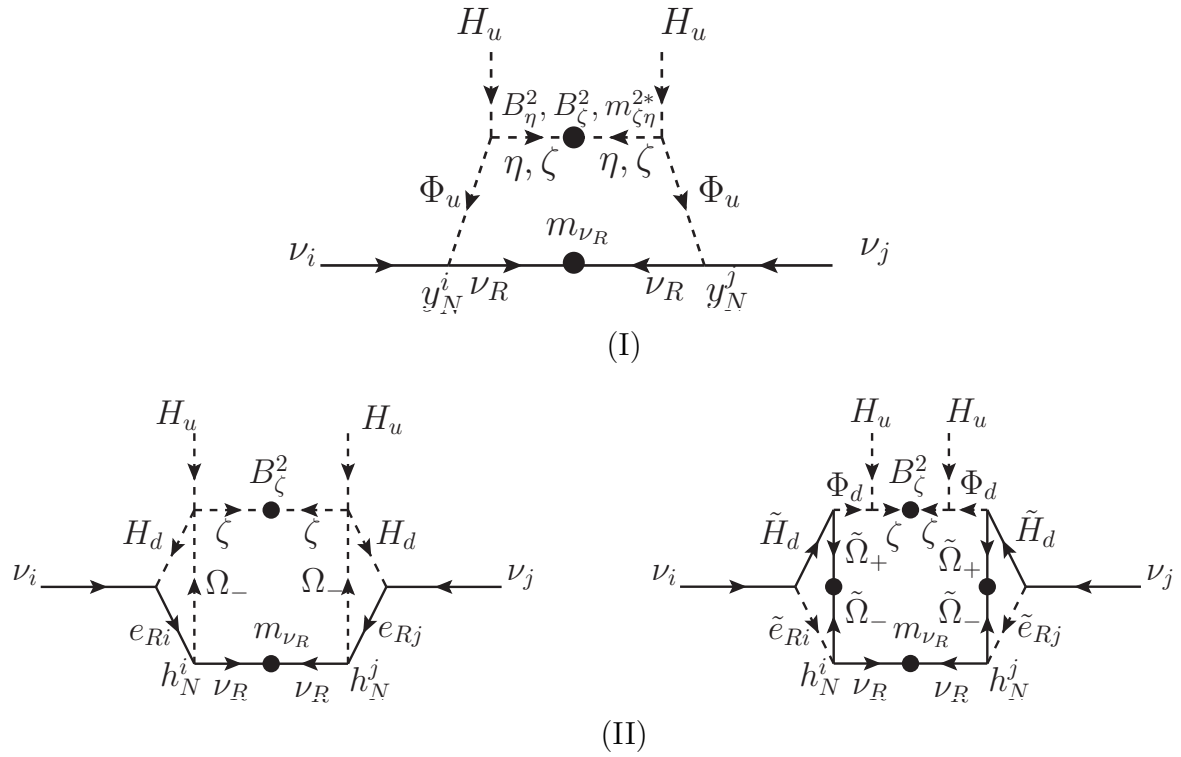

Figure 1: (I) A one-loop diagram and (II) three-loop diagrams which contribute to the neutrino mass matrix.

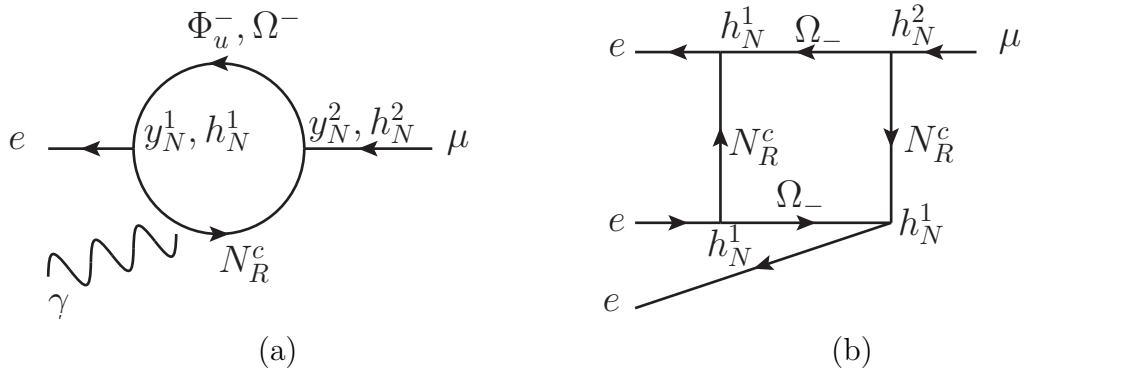

Figure 2: (a) The contribution to the $\mu \to e\gamma$ process and (b) the box contribution to the $\mu \to eee$ process from the Z_2-odd particles with the RH neutrino.

independent constraint on the parameter space. If the MSSM slepton sector has flavour mixing, there will be additional contributions to the LFV.

In the low-energy effective theory of our model, two different discrete symmetries: *i.e.*, both the Z_2-parity and the R-parity are unbroken. Therefore, there can be three kinds of DM candidates, which are the lightest particles with the parity assignments of $(+,-)$, $(-,+)$, and $(-,-)$ for (Z_2-parity, R-parity). The observed value of the thermal relic abundance of DM should be explained by the summation of the relic abundances of these DM candidates. If one of the three particle is heavy enough to decay into the other two particles, the heaviest one cannot be a DM, and only the other two candidates can compose the DM relic abundance. In multi-component DM case[33], not only the pair annihilation processes of each DM candidates but also the conversion process from one DM particle to the other DM particle can play significant role in the evaluation of the relic abundance.

4. Benchmark scenario

We discuss a benchmark scenario of our model, where the strong 1stOPT is realized as $\varphi_c/T_c \gtrsim 1$, the neutrino oscillation data can be explained with satisfying the constraints from the LFV processes, and the DM relic abundance can be also reproduced, simultaneously. The input parameters of the benchmark scenario are listed in Table 3. The predictions in the benchmark scenario are shown in Table 4, and the mass spectrum for the relevant particles in the benchmark scenario is shown in Fig. 3. We here discuss the reason of our choice for the benchmark scenario and its predictions.

The Lagrangian of the Z_2-even Higgs sector is the same as the nMSSM. The Z_2-odd sector affects the Z_2-even Higgs sector only by the loop effects. The SM-like Higgs boson mass in our model is estimated as

$$m_h^2 \simeq m_Z^2 \cos^2 2\beta + \frac{\lambda^2 v^2}{2} \sin^2 2\beta + \delta m_h(\text{loop}) \,, \tag{10}$$

where the $\delta m_h(\text{loop})$ denotes the loop corrections. If the value of $\tan\beta$ is small, the tree level mass of the SM-like Higgs boson becomes too large because of $\lambda \simeq 1.8$, and the measured value $m_h = 126$ GeV cannot be reproduced. Therefore, we take $\tan\beta = 15$ in the benchmark scenario. In this case, the loop correction $\delta m_h(\text{loop})$ plays an important role in the determination of the SM-like Higgs boson mass because the second term in Eq. (10) is negligibly small. The significant loop corrections on the Higgs mass are from the loop contributions of the top and stop fields as in the MSSM, as well as from the loop diagrams with Z_2-odd fields which has large coupling constant with the SM-like Higgs boson.

To realise $\varphi_c/T_c > 1$, non-decoupling effect of the Z_2-odd particles is necessary. The condition $\varphi_c/T_c \gtrsim 1$ requires the large coupling constant λ as $\lambda \simeq 1.8$ which corresponds to the cut-off scale of $\Lambda_H \sim 5$ TeV. In our model, there are two possible combinations of Z_2-odd particles which give non-decoupling effects on φ_c/T_c. One possible way is that φ_c/T_c is enhanced by the non-decoupling loop effect of the scalar component of Ω_- and the charged scalar component of Φ_u. This choice is the same as the one discussed in Ref. [11]. The other is that the enhancement of φ_c/T_c is caused by the non-decoupling loop effect of

Table 3: The input parameters for the benchmark scenario. In the list, $\bar{m}^2_{\phi_i} = m^2_{\phi_i} + |\mu_i|^2$ are taken as input parameters, where $\mu_i = \mu_\Phi$ for $\phi_i = \Phi_u, \Phi_d$, and $\mu_i = \mu_\Omega$ for $\phi_i = \Omega_+, \Omega_-, \zeta, \eta$.

λ, $\tan\beta$, and μ-terms
$\lambda = 1.8$ ($\Lambda_H = 5$ TeV) $\quad \tan\beta = 15 \quad \mu = 250$ GeV $\quad \mu_\Phi = 550$ GeV $\quad \mu_\Omega = -550$ GeV
Z_2-even Higgs sector
$m_h = 126$ GeV $\quad m_{H^\pm} = 990$ GeV $\quad m_N^2 = (1050\text{ GeV})^2 \quad A_N = 2900$ GeV
Z_2-odd Higgs sector
$\bar{m}^2_{\Phi_u} = \bar{m}^2_{\Omega_-} = (75\text{ GeV})^2 \quad \bar{m}^2_{\Phi_d} = \bar{m}^2_{\Omega_+} = \bar{m}^2_\zeta = (1500\text{ GeV})^2 \quad \bar{m}^2_\eta = (2000\text{ GeV})^2$
$B_\Phi = B_\Omega = A_\zeta = A_\eta = A_{\Omega^+} = A_{\Omega^-} = m^2_{\zeta\eta} = 0 \quad B^2_\zeta = (1400\text{ GeV})^2 \quad B^2_\eta = (700\text{ GeV})^2$
RH neutrino and RH sneutrino sector
$m_{\nu_R} = 63$ GeV $\quad m_{\tilde{\nu}_R} = 65$ GeV $\quad \kappa = 0.9$
$y_N = (3.28i, 6.70i, 1.72i) \times 10^{-6} \quad h_N = (0, 0.227, 0.0204)$
Other SUSY SM parameters
$m_{\tilde{W}} = 500$ GeV $\quad m_{\tilde{q}} = m_{\tilde{\ell}} = 5$ TeV

the scalar component of η and the charged scalar component of Φ_u. However, for the latter case, the LFV constraint is too severe to avoid the present upper bound on $\mathrm{B}(\mu \to e\gamma)$ if only one RH neutrino is introduced. In the benchmark scenario, we take the first possibility. Therefore, the 1stOPT is enhanced as $\varphi_c/T_c = 1.3$ by the non-decoupling loop contributions of the two charged scalar particles Φ_1^- and Φ_2^-, whose main components come from the scalar components of $(\Phi_u^+)^*$ and Ω_-, respectively. In this case, the masses of these scalar particles are mainly determined by the vev contributions instead of their soft breaking mass parameters.

The non-decoupling effects of the loop contributions by $\Phi_1^\pm$ and $\Phi_2^\pm$ simultaneously affect the predictions on both the branching ratio of $h \to \gamma\gamma$ process and the triple Higgs boson coupling constant λ_{hhh}[9]. One can find the minus 20% deviation on $\mathrm{B}(h \to \gamma\gamma)$ from the SM prediction. At the present, the LHC data with $\sqrt{s} = 7$ TeV and $\sqrt{s} = 8$ TeV have determined the $\mathrm{B}(h \to \gamma\gamma)$ with 50% accuracy[34], and the accuracy will be improved to 10% at the HL-LHC with the luminosity of 3000fb^{-1}[31]. Therefore the model can be tested by measuring the branching ratio of $h \to \gamma\gamma$ at the HL-LHC. As for the λ_{hhh}, the plus 20% deviation from the SM prediction is predicted, and it is testable at the ILC with $\sqrt{s} = 1$ TeV with the luminosity of 2.5 ab^{-1} where the λ_{hhh} is measured with 13% accuracy[32].

Two finite mass eigenvalues can be obtained with only one RH neutrino. In the benchmark scenario, the solar neutrino mass difference is mainly induced by the one-loop contribution shown in Fig. 1-(I), and the atmospheric neutrino mass difference is dominated by the three-loop contributions shown in Fig. 1-(II). As shown in Table 4, the predicted mass

Table 4: Predictions of the benchmark points given in Table 3.

Non-decoupling effects
$\varphi_c/T_c = 1.3 \quad \lambda_{hhh}/\lambda_{hhh}\vert_{\rm SM} = 1.2 \quad {\rm B}(h \to \gamma\gamma)/{\rm B}(h \to \gamma\gamma)\vert_{\rm SM} = 0.78$
Neutrino masses and the mixing angles
$(m_1, m_2, m_3) = (0, 0.0084\ {\rm eV}, 0.0050\ {\rm eV}) \quad \sin^2\theta_{12} = 0.32 \quad \sin^2\theta_{23} = 0.50 \quad \vert\sin\theta_{13}\vert = 0.14$
LFV processes
${\rm B}(\mu \to e\gamma) = 3.6 \times 10^{-13} \quad {\rm B}(\mu \to eee) = 5.6 \times 10^{-16}$
Relic abundance of the DM
$\Omega_{\nu_R}h^2 = 0.055 \quad \Omega_{\tilde{\nu}_R}h^2 = 0.065 \quad \Omega_{\rm DM} = \Omega_{\nu_R}h^2 + \Omega_{\tilde{\nu}_R}h^2 = 0.12$

eigenvalues and the mixing angles are consistent with their allowed region which is obtained from the global fitting analysis of the neutrino oscillation data as[35]

$$
\begin{aligned}
&2.28 \times 10^{-3}\ {\rm eV}^2 < |m_3^2 - m_1^2| < 2.70 \times 10^{-3}\ {\rm eV}^2\ , \\
&7.0 \times 10^{-5}\ {\rm eV}^2 < m_2^2 - m_1^2 < 8.1 \times 10^{-5}{\rm eV}^2, \\
&0.27 < \sin^2\theta_{12} < 0.34\ , \quad 0.34 < \sin^2\theta_{23} < 0.67\ , \quad 0.016 < \sin^2\theta_{13} < 0.030\ .
\end{aligned} \tag{11}
$$

The light neutrino mass pattern in our benchmark is the normal hierarchy ($m_1 < m_2 < m_3$). It is difficult to reproduce the inverted hierarchical pattern ($m_3 < m_1 < m_2$) with satisfying the LFV constraint when only one RH neutrino is introduced.

The experimental upper bound on the branching ratio ${\rm B}(\mu \to e\gamma)$ gives a severe constraint on the parameter space. In the benchmark scenario, though the contribution to the $\mu \to e\gamma$ process is suppressed to some extent by taking $h_N^1 = 0$, the predicted value of the branching ratio of $\mu \to e\gamma$ as ${\rm B}(\mu \to e\gamma) = 3.6 \times 10^{-13}$ is just below the present upper limit such as ${\rm B}(\mu \to e\gamma) \simeq 5.7 \times 10^{-13}$, which is given by the MEG experiment[28]. The box diagram contribution to $\mu \to eee$ in the benchmark scenario is negligible compared to the penguin and dipole contributions because of $h_N^1 = 0$. Therefore, the predicted branching ratio of $\mu \to eee$ easily satisfies the experimental upper limit such as ${\rm B}(\mu \to eee) \simeq 10^{-12}$[36].

There are three DM candidates in our model; *i.e.*, the lightest particles with the parity assignments of $(+,-)$, $(-,+)$, and $(-,-)$ for the (Z_2-parity, R-parity). In our benchmark scenario, the lightest $(+,-)$, $(-,+)$, and $(-,-)$ particles are identical to the lightest Z_2-even neutralino, the RH neutrino and the RH sneutrino, respectively. One may consider another possibility for the lightest $(-,+)$ and $(+,-)$ particles such as Φ_1 and $\tilde{\Phi}_1$. However, different from the RH neutrino and RH sneutrino, the other Z_2-odd particle have gauge interactions in addition to the large coupling constant with the SM-like Higgs boson. Therefore, the scattering cross section with the proton is too large to avoid the constraint from the direct detection experiments such as the XENON100 experiment[27] and the LUX experiment[26].

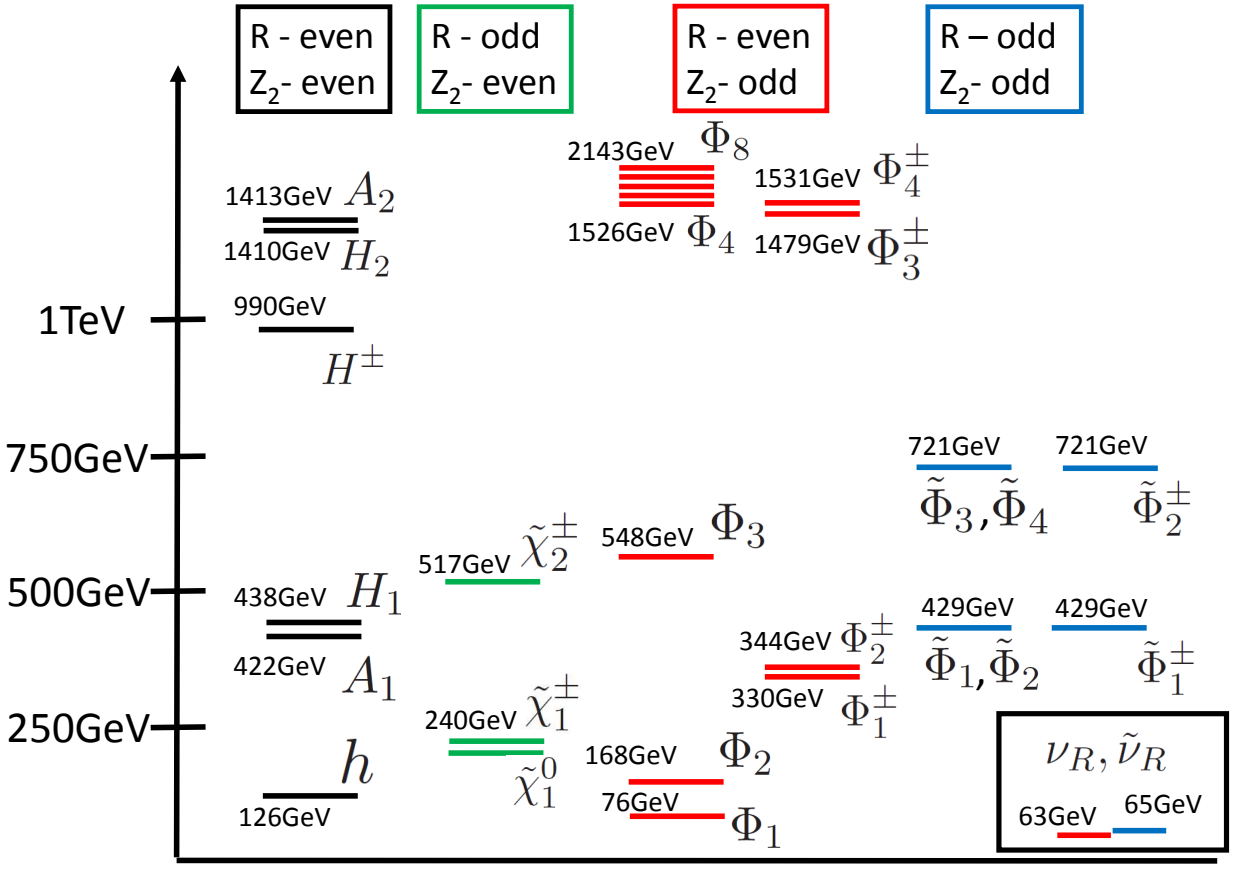

Figure 3: The mass spectrum of the relevant particles in the benchmark scenario given in Table 3.

In the benchmark scenario, the lightest Z_2-even neutralino $\tilde{\chi}_1^0$ is heavy enough to decay into the RH neutrino and the RH sneutrino, and it cannot be a DM candidate. Consequently, there are only two DM candidate; *i.e.*, the RH neutrino and the RH sneutrino. In Section 5, we show the brief discussion of the numerical analysis of the relic abundance in this two component DM system. The annihilation and the conversion processes of the RH neutrino and the RH sneutrino are dominated by the exchange of the Z_2-even singlet scalar N which mixes to the SM-like Higgs boson. The diagrams of the annihilation processes are shown in Fig. 4. As shown in Fig. 5, in order to reproduce the observed DM relic abundance $\Omega_{\rm DM}h^2 = \Omega_{\nu_R}h^2 + \Omega_{\tilde{\nu}_R}h^2 \simeq 0.12$ [3], the masses of the RH neutrino and the RH sneutrino should be about one half of the SM-like Higgs boson mass, $m_{\nu_R} \simeq m_{\tilde{\nu}_R} \simeq m_h/2$. In this case, the effect of the s-channel resonance can enhance the annihilation processes enough to reproduce the observed relic abundance of DM. The coupling between the DM particles and the SM-like Higgs boson is determined by the combination of the coupling constant κ and the mixing angles in the Z_2-even and CP-even neutral scalar sector. In order to enhance the annihilation process in this way, the mixing among the scalar components of N and H_d has to be large, and the SM-like Higgs boson should contain the non-negligible component from

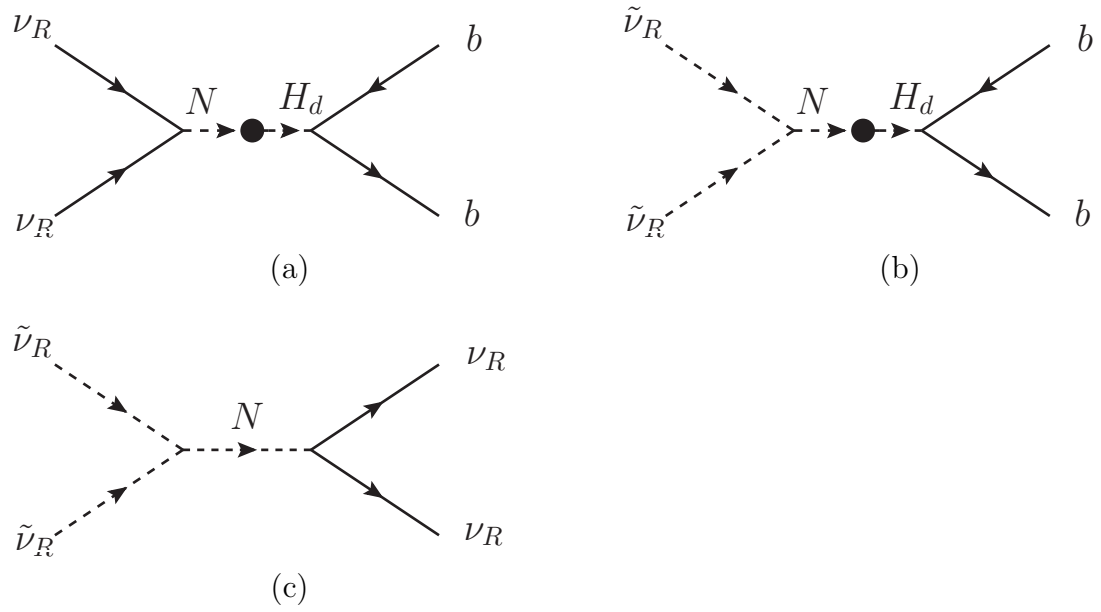

Figure 4: The main annihilation processes of (a) the RH neutrino and (b) the RH sneutrino and (c) the conversion process from the RH neutrino pair to the RH sneutrino pair.

the scalar component of the singlet N.

Since both the RH neutrino and the RH sneutrino are gauge singlet fields, they scatter off the proton only through the Higgs exchange diagram, and the scattering cross section with the proton is suppressed by the Yukawa coupling constant of light quarks such as u, d, and s. Then the cross section is far below the current limits by direct detection experiments[26, 27].

If the Z_2-even neutralino is too light to decay into the RH neutrino and the RH sneutrino, the neutralino $\tilde{\chi}_1^0$ can also be a DM candidate in addition to the RH neutrino and the RH sneutrino. In this case, some additional mechanism to accelerate the annihilation of $\tilde{\chi}_1^0$ is necessary to reproduce the observed relic abundance of DM; *e.g.*, co-annihilation with stau and so on.

Our simple benchmark scenario given in Table 3 can explain the DM relic abundance, the neutrino oscillation data with satisfying the experimental bound from the LFV process and with retaining the strong 1stOPT for successful electroweak baryogenesis by introducing only one RH neutrino superfield.

5. Analysis of the DM relic abundance

We here briefly show how the relic abundance is numerically evaluated with the two DM particles; *i.e.*, the RH neutrino and the RH sneutrino. The relic abundance of DM in this scenario is the summation of the relic abundances of the RH neutrino and the RH sneutrino.

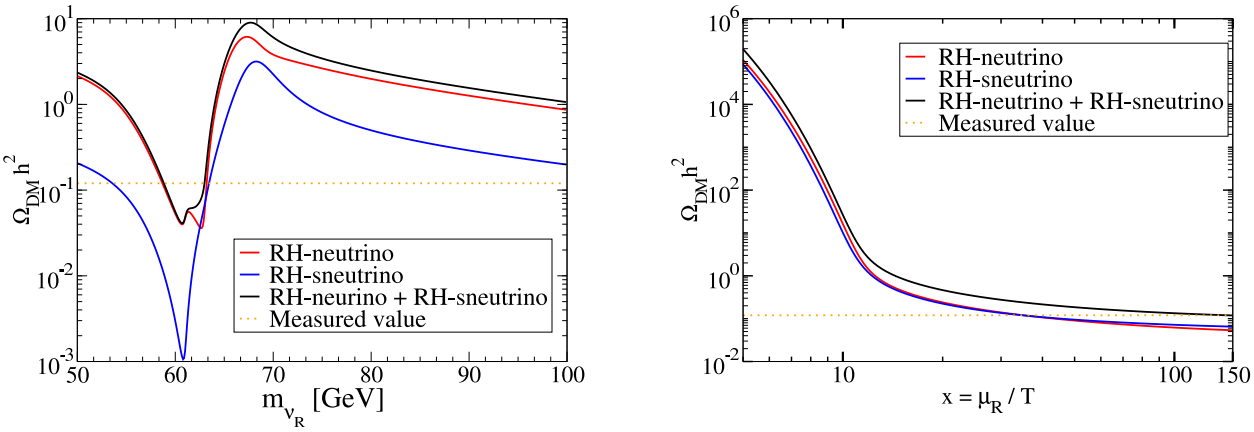

Figure 5: (a) The prediction on the thermal relic densities of the RH neutrino and the RH sneutrino as functions of the RH neutrino mass m_{ν_R}. The sneutrino mass is taken as $m_{\tilde{\nu}_R} = m_{\nu_R} + 2\text{GeV}$. The other parameters are the same as ones in Table 3. (b) The behaviour of the thermal relic abundances in the benchmark scenario: *i.e.*, the mass of the RH neutrino and the RH sneutrino are fixed as $m_{\nu_R} = 63$ GeV and $m_{\tilde{\nu}_R} = 65$ GeV.

These relic abundances are evaluated by using the coupled Boltzmann equations as

$$\begin{aligned}
\frac{dY}{dx} =& 0.264 g_*^{1/2} \left(\frac{\mu_R M_P}{x^2}\right) \\
&\times \left\{ -\langle\sigma_\nu v\rangle \left(Y^2 - Y_{\rm eq}^2\right) - \langle\sigma_{\nu\tilde{\nu}} v\rangle \left(Y^2 - \tilde{Y}^2 \frac{Y_{\rm eq}^2}{\tilde{Y}_{\rm eq}^2}\right) + \langle\sigma_{\tilde{\nu}\nu} v\rangle \left(\tilde{Y}^2 - Y^2 \frac{\tilde{Y}_{\rm eq}^2}{Y_{\rm eq}^2}\right) \right\} , \\
\frac{d\tilde{Y}}{dx} =& 0.264 g_*^{1/2} \left(\frac{\mu_R M_P}{x^2}\right) \\
&\times \left\{ -\langle\sigma_{\tilde{\nu}} v\rangle \left(\tilde{Y}^2 - \tilde{Y}_{\rm eq}^2\right) - \langle\sigma_{\tilde{\nu}\nu} v\rangle \left(\tilde{Y}^2 - Y^2 \frac{\tilde{Y}_{\rm eq}^2}{Y_{\rm eq}^2}\right) + \langle\sigma_{\nu\tilde{\nu}} v\rangle \left(\tilde{Y}^2 - Y^2 \frac{\tilde{Y}_{\rm eq}^2}{Y_{\rm eq}^2}\right) \right\} . \quad (12)
\end{aligned}$$

In the above expressions, Y and $\tilde{Y}$ denote the ratio of the particle number density to the entropy density for the RH neutrino and the RH sneutrino, respectively. $Y_{\rm eq}$ and $\tilde{Y}_{\rm eq}$ are the equilibrium numbers for the Y and $\tilde{Y}$, x is the dimensionless inverse temperature $x = \frac{\mu_R}{T}$ with μ_R being the reduced mass of the two component system as $\mu_R^{-1} = m_{\nu_R}^{-1} + m_{\tilde{\nu}_R}^{-1}$, $g_*^{1/2}$ is a parameter for the effective degrees of freedom in the thermal equilibrium, and M_P is the Planck mass. In the thermal averaged cross sections $\langle\sigma v\rangle$, the cross sections σ_ν, $\sigma_{\tilde{\nu}}$, $\sigma_{\nu\tilde{\nu}}$, and $\sigma_{\tilde{\nu}\nu}$ are relevant to the processes such as $\nu_R\nu_R \to XX$ (X denotes a generic SM fermion particles.), $\tilde{\nu}_R\tilde{\nu}_R \to XX$, $\nu_R\nu_R \to \tilde{\nu}_R\tilde{\nu}_R$ and $\tilde{\nu}_R\tilde{\nu}_R \to \nu_R\nu_R$, respectively. In this benchmark scenario, $\sigma_{\nu\tilde{\nu}}$ is kinematically suppressed. The relic densities of the RH neutrino and the

Table 5: The deviations in the coupling constants from the SM predictions in the benchmark scenario.

κ_W	κ_Z	κ_u	κ_d	κ_ℓ	κ_γ	$\lambda_{hhh}/\lambda_{hhh}^{\rm SM}$
0.990	0.990	0.990	0.978	0.978	0.88	1.2

RH sneutrino are evaluated from the frozen out values of Y and $\tilde{Y}$ as

$$\Omega_{\nu_R}h^2 = 2.74\times 10^8 \left(\frac{m_{\nu_R}}{1\text{GeV}}\right) Y \ , \quad \Omega_{\tilde{\nu}_R}h^2 = 2.74\times 10^8 \left(\frac{m_{\tilde{\nu}_R}}{1\text{GeV}}\right) \tilde{Y} \ . \tag{13}$$

The numerical behaviour of the thermal relic abundance of the RH neutrino and the RH sneutrino in the benchmark scenario is shown in Fig. 5-(b).

6. Discussion

For electroweak baryogenesis, we have focused on the strong 1stOPT which is one of the necessary conditions for successful baryogenesis. Towards a complete analysis of generation of the BAU, the CP violating phases should also be taken into account. Since it is known that the CP violation in the SM is not enough for the successful baryogenesis[37], new CP violating source is required to be introduced. In the SUSY model, several new CP violating phases can be introduced, some of which can contribute to the baryogenesis[38]. With such CP phases, the BAU in the electroweak baryogenesis scenario is numerically evaluated in the MSSM[39]. In our model, by introducing CP phase to the model in the similar way to the case of the MSSM, we expect to reproduce the measured amount of the BAU, if the 1stOPT is strong enough. However, it should be carefully checked if introducing such a CP phase does not conflict with the experimental constraints as the bounds on the neutron electric dipole moment and so on[39]. The complete analysis for getting the BAU in our model will be performed elsewhere.

Let us discuss the testability of our model. In the benchmark scenario, Z_2-odd scalars H_1 and A_1 are rather light as $m_{H_1} = 438$ GeV and $m_{A_1} = 422$ GeV. Such masses for $\tan\beta = 15$ can be easily searched at the LHC with $\sqrt{s} = 14$ TeV[40]. When they are discovered, they may look like the heavy Higgs and the CP-odd Higgs in the MSSM or the two Higgs doublet model. On the other hand, the Z_2-even charged Higgs is not degenerate to the H_1 and A_1 in the benchmark scenario as $m_{H^\pm} = 990$ GeV. This mass spectrum is quite different from the MSSM in which it is known a mass relation is satisfied $m_{H^\pm}^2 = m_A^2 + m_W^2$ for the charged Higgs mass $m_{H^\pm}$ and the CP-odd Higgs mass m_A. Therefore our model can be distinguished from the MSSM. In addition, their property will be precisely measured at the ILC with $\sqrt{s} = 1$ TeV. Both H_1 and A_1 in the benchmark scenario are mixture of the doublet and the singlet. The precision measurements of these heavy state; *e.g.*, coupling measurement with bottom quarks and tau leptons, also provide enough information to distinguish our model from the MSSM, the two Higgs doublet model and so on.

Since such a mass spectrum and properties from the mixture with the singlet state are found in the nMSSM too, it is hard to distinguish our model from the nMSSM by

these measurements only. However, in our model, the Z_2-odd sector affects the Z_2-even Higgs sector through the non-decoupling loop effect, which will be explored by precision measurements of the SM-like Higgs boson at future collider experiments. Table 5 shows the deviations from the SM prediction in the coupling constants of the SM-like Higgs boson. The deviations are parametrised by the scale factors $\kappa_\phi \equiv g_{h\phi\phi}/g^{\rm SM}_{h\phi\phi}$ for $h\phi^{(*)}\phi$ couplings ($\phi = Z, W, u, d, \ell, \gamma$). The deviations in κ_W, κ_Z, κ_u, κ_d and κ_ℓ mainly originate from the mixture between the SM-like Higgs boson and the singlet scalar component of N, while the deviations in κ_γ and the triple Higgs boson coupling $\lambda_{hhh}/\lambda^{\rm SM}_{hhh}$ are caused by the non-decoupling effect of Z_2-odd particles. Therefore, the deviations in κ_γ and $\lambda_{hhh}/\lambda^{\rm SM}_{hhh}$ can distinguish our model from the nMSSM. It is expected that the deviation in κ_γ can be tested with a few percent accuracy at the HL-LHC with the luminosity of 3000fb^{-1}[31]. For λ_{hhh}, the ILC with $\sqrt{s} = 1$ TeV with the luminosity of 2.5 ab^{-1} can measure the positive deviation at most the 13% accuracy[32]. Therefore, our model can be tested by measuring the self coupling constant of the SM-like Higgs boson.

Even if H_1 and A_1 are heavier so that they are not discovered at the LHC with $\sqrt{s} =$ 14 TeV, the precision measurements of the SM-like Higgs boson are very powerful tool to explore the framework of our model. We can consider a benchmark case with much heavier H_1 and A_1, where LFV constraint becomes more severe, but it is avoidable by introducing the second RH neutrino superfield. In such a benchmark with heavier H_1 and A_1, a few percent of deviations can appear in κ_W, κ_Z, κ_u, κ_d and κ_ℓ caused by the mixture of the SM-like Higgs boson and the singlet scalar N. Precision measurements of these scale factors give us a strong hint to distinguish our model from the MSSM.

The existence of light Z_2-odd particles characterize our benchmark scenario so that the signals in the direct search of the Z_2-odd particles are very important. In the literature[41], collider phenomenology of Z_2-odd doublet scalars have been discussed. In a specific case, the Z_2-odd scalars might be discovered at the LHC by using the cascade decays of heavier particles. However, in general, it is not easy to discover them at the LHC because these Z_2-odd particles are colour singlet particles. On the other hand, the ILC is a strong tool for not only discovering them but also for determining their masses and quantum numbers. As discussed in Ref. [42], the mass of a neutral Z_2-odd doublet-like scalar can be determined in more than 2 GeV accuracy, and a Z_2-odd charged scalar mass can be measured in a few GeV accuracy at the ILC with $\sqrt{s} = 250$ GeV.

In our model, significant size of the LFV is unavoidable, because the origin of the neutrino mass in our model is at the TeV scale. Actually, in the benchmark scenario, the prediction on the branching ratio of $\mu \to e\gamma$ is just below the present upper limit. Therefore, a signal of $\mu \to e\gamma$ is strongly expected to be found in a future experiment such as an upgrade version of the MEG experiment [43], whose sensitivity on the $\mu \to e\gamma$ will reach B($\mu \to e\gamma$) $< 10^{-14}$.

7. Summary

We propose a simple model to explain the problems which cannot be explained in the SM; *i.e.*, tiny neutrino mass, DM and baryogenesis. The model is based on the idea that the extended Higgs sector appears as a low-energy effective theory of a SUSY gauge theory

with confinement. We have considered the $SU(2)_H$ gauge symmetry with three flavours of fundamental representations and a new discrete Z_2 symmetry. A Z_2-odd RH neutrino superfield is also introduced. In the low-energy effective theory, SUSY extended Higgs sector appears, where there are several Z_2-odd composite superfields. When the confinement scale is of the order of ten TeV, electroweak phase transition can be sufficiently of first order for successful electroweak baryogenesis by the non-decoupling effect of the Z_2-odd particles by the non-decoupling effect of the Z_2-odd particles. In addition to the lightest R-parity odd DM candidate, the lightest Z_2-odd particle can be a new candidate for DM. Neutrino masses and mixings can be explained by the quantum effects of Z_2-odd fields via the one-loop and three-loop diagrams. We have found a simple benchmark scenario of the model, where all the constraints from neutrino, DM, LFV and LHC data are satisfied. We have also discussed its testability at future collider experiments and LFV experiments.

Acknowledgement

We would like to thank Toshifumi Yamada for useful discussions. This work was supported in part by Grant-in-Aid for Scientific Research, Japan Society for the Promotion of Science (JSPS) and Ministry of Education, Culture, Sports, Science and Technology, Nos. 22244031 (S.K.), 23104006 (S.K.), 23104011 (T.S.) and 24340046 (S.K. and T.S.). The work of N.M. was supported in part by the Sasakawa Scientific Research Grant from the Japan Science Society.

References

[1] G. Aad *et al.* [ATLAS Collaboration], Phys. Lett. B **710** (2012) 49; S. Chatrchyan *et al.* [CMS Collaboration], Phys. Lett. B **710** (2012) 26.

[2] Y. Fukuda *et al.* [Super-Kamiokande Collaboration], Phys. Rev. Lett. **81** (1998) 1562; Q. R. Ahmad *et al.* [SNO Collaboration], Phys. Rev. Lett. **89** (2002) 011301; K. Eguchi *et al.* [KamLAND Collaboration], Phys. Rev. Lett. **90** (2003) 021802; F. P. An *et al.* [DAYA-BAY Collaboration], Phys. Rev. Lett. **108** (2012) 171803; J. K. Ahn *et al.* [RENO Collaboration], Phys. Rev. Lett. **108** (2012) 191802; K. Abe *et al.* [T2K Collaboration], Phys. Rev. Lett. **112** (2014) 061802.

[3] G. Hinshaw *et al.* [WMAP Collaboration], Astrophys. J. Suppl. **208** (2013) 19.

[4] M. Fukugita and T. Yanagida, Phys. Lett. B **174** (1986) 45; I. Affleck and M. Dine, Nucl. Phys. B **249** (1985) 361; M. Dine, L. Randall and S. D. Thomas, Nucl. Phys. B **458** (1996) 291 [hep-ph/9507453].

[5] V. A. Kuzmin, V. A. Rubakov and M. E. Shaposhnikov, Phys. Lett. B **155** (1985) 36; A. G. Cohen, D. B. Kaplan and A. E. Nelson, Ann. Rev. Nucl. Part. Sci. **43** (1993) 27; M. Quiros, Helv. Phys. Acta **67** (1994) 451; V. A. Rubakov and M. E. Shaposhnikov, Usp. Fiz. Nauk **166** (1996) 493 [Phys. Usp. **39** (1996) 461]; K. Funakubo, Prog. Theor. Phys. **96** (1996) 475; M. Trodden, Rev. Mod. Phys. **71** (1999) 1463; W. Bernreuther, Lect. Notes Phys. **591** (2002) 237; J. M. Cline, hep-ph/0609145; D. E. Morrissey and M. J. Ramsey-Musolf, New J. Phys. **14** (2012) 125003.

[6] M. Joyce, T. Prokopec and N. Turok, Phys. Rev. D **53** (1996) 2930; M. Joyce, T. Prokopec and N. Turok, Phys. Rev. D **53** (1996) 2958; J. M. Cline, K. Kainulainen and A. P. Vischer, Phys. Rev. D **54** (1996) 2451; J. M. Cline and P. -A. Lemieux, Phys. Rev. D **55** (1997) 3873; L. Fromme, S. J. Huber and M. Seniuch, JHEP **0611** (2006) 038; A. Kozhushko and V. Skalozub, Ukr. J. Phys. **56** (2011) 431.

[7] M. S. Carena, M. Quiros and C. E. M. Wagner, Phys. Lett. B **380** (1996) 81 M. S. Carena, M. Quiros, M. Seco and C. E. M. Wagner, Nucl. Phys. B **650** (2003) 24; C. Lee, V. Cirigliano and M. J. Ramsey-Musolf, Phys. Rev. D **71** (2005) 075010; V. Cirigliano, M. J. Ramsey-Musolf, S. Tulin and C. Lee, Phys.

Rev. D **73** (2006) 115009; T. Konstandin, T. Prokopec, M. G. Schmidt and M. Seco, Nucl. Phys. B **738** (2006) 1; D. J. H. Chung, B. Garbrecht, M. J. Ramsey-Musolf and S. Tulin, Phys. Rev. Lett. **102** (2009) 061301; K. Funakubo, S. Tao and F. Toyoda, Prog. Theor. Phys. **109** (2003) 415; M. Carena, G. Nardini, M. Quiros and C. E. M. Wagner, Nucl. Phys. B **812** (2009) 243; K. Funakubo and E. Senaha, Phys. Rev. D **79** (2009) 115024;

[8] S. Kanemura, E. Senaha and T. Shindou, Phys. Lett. B **706** (2011) 40

[9] S. Kanemura, Y. Okada and E. Senaha, Phys. Lett. B **606** (2005) 361

[10] L. D. Landau, in "Niels Bohr and the Development of Physics", ed. W. Pauli (Pergamon Press, London, 1955).

[11] S. Kanemura, E. Senaha, T. Shindou and T. Yamada, JHEP **1305** (2013) 066.

[12] S. Kanemura, T. Shindou and T. Yamada, Phys. Rev. D **86** (2012) 055023.

[13] P. Minkowski, Phys. Lett. B **67** (1977) 421; M. Gell-Mann, P. Ramond, and R. Slansky in *Supergravity*, p. 315, edited by F. Nieuwenhuizen and D. Friedman, North Holland, Amsterdam, 1979; T. Yanagida, Proc. of the *Workshop on Unified Theories and the Baryon Number of the Universe*, edited by O. Sawada and A. Sugamoto, KEK, Japan 1979; Prog. Theor. Phys. **64** (1980) 1103; S. L. Glashow, in *Proc. of the Cargése Summer Institute on Quarks and Leptons*, Cargése, July 9-29, 1979, eds. M. Lévy et al. , (Plenum, 1980, New York), p707; R. N. Mohapatra and G. Senjanovic, Phys. Rev. Lett. **44**, (1980) 912.

[14] J. Schechter and J. W. F. Valle, Phys. Rev. D **22** (1980) 2227; T. P. Cheng and L. F. Li, Phys. Rev. D **22** (1980) 2860; M. Magg and C. Wetterich, Phys. Lett. B **94** (1980) 61; C. Wetterich, Nucl. Phys. B **187** (1981) 343; G. Lazarides, Q. Shafi and C. Wetterich, Nucl. Phys. B **181** (1981) 287; R. N. Mohapatra and G. Senjanovic, Phys. Rev. D **23** (1981) 165.

[15] R. Foot, H. Lew, X. G. He and G. C. Joshi, Z. Phys. C **44** (1989) 441; E. Ma, Phys. Rev. Lett. **81** (1998) 1171.

[16] A. Zee, Phys. Lett. B **93** (1980) 389 [Erratum-ibid. B **95** (1980) 461].

[17] E. Ma, Phys. Rev. D **73** (2006) 077301.

[18] M. Aoki, S. Kanemura and O. Seto, Phys. Rev. Lett. **102** (2009) 051805; M. Aoki, S. Kanemura and O. Seto, Phys. Rev. D **80** (2009) 033007.

[19] M. Aoki, S. Kanemura and K. Yagyu, Phys. Rev. D **83** (2011) 075016.

[20] A. Zee, Nucl. Phys. B **264** (1986) 99; K. S. Babu, Phys. Lett. B **203** (1988) 132.

[21] M. Aoki, S. Kanemura, T. Shindou and K. Yagyu, JHEP **1007** (2010) 084 [Erratum-ibid. **1011** (2010) 049].

[22] L. M. Krauss, S. Nasri and M. Trodden, Phys. Rev. D **67** (2003) 085002.

[23] K. A. Intriligator and N. Seiberg, Nucl. Phys. Proc. Suppl. **45BC** (1996) 1.

[24] R. Harnik, G. D. Kribs, D. T. Larson and H. Murayama, Phys. Rev. D **70** (2004) 015002.

[25] S. Kanemura, N. Machida, T. Shindou and T. Yamada, Phys. Rev. D **89** (2014) 013005.

[26] D. S. Akerib *et al.* [LUX Collaboration], Phys. Rev. Lett. **112** (2014) 091303.

[27] E. Aprile *et al.* [XENON100 Collaboration], Phys. Rev. Lett. **107** (2011) 131302.

[28] J. Adam *et al.* [MEG Collaboration], Phys. Rev. Lett. **110** (2013) 20, 201801.

[29] H. Georgi, A. Manohar and G. W. Moore, Phys. Lett. B **149** (1984) 234; H. Georgi and L. Randall, Nucl. Phys. B **276** (1986) 241; M. A. Luty, Phys. Rev. D **57** (1998) 1531; A. G. Cohen, D. B. Kaplan and A. E. Nelson, Phys. Lett. B **412** (1997) 301.

[30] C. Panagiotakopoulos and K. Tamvakis, Phys. Lett. B **446** (1999) 224; C. Panagiotakopoulos and K. Tamvakis, Phys. Lett. B **469** (1999) 145; C. Panagiotakopoulos and A. Pilaftsis, Phys. Rev. D **63** (2001) 055003; A. Dedes, C. Hugonie, S. Moretti and K. Tamvakis, Phys. Rev. D **63** (2001) 055009.

[31] ATLAS Collaboration, ATL-PHYS-PUB-2012-001; ATL-PHYS-PUB-2012-004.

[32] H. Baer, T. Barklow, K. Fujii, Y. Gao, A. Hoang, S. Kanemura, J. List and H. E. Logan *et al.*, arXiv:1306.6352 [hep-ph]; D. M. Asner, T. Barklow, C. Calancha, K. Fujii, N. Graf, H. E. Haber, A. Ishikawa and S. Kanemura *et al.*, arXiv:1310.0763 [hep-ph].

[33] M. Aoki, M. Duerr, J. Kubo and H. Takano, Phys. Rev. D **86** (2012) 076015.

[34] ATLAS Collaboration, ATLAS-CONF-2013-012; CMS Collaboration, CMS-PAS-HIG-13-016.

[35] G. L. Fogli, E. Lisi, A. Marrone, D. Montanino, A. Palazzo and A. M. Rotunno, Phys. Rev. D **86**

(2012) 013012; M. C. Gonzalez-Garcia, M. Maltoni, J. Salvado and T. Schwetz, JHEP **1212** (2012) 123.
[36] U. Bellgardt *et al.* [SINDRUM Collaboration], Nucl. Phys. B **299** (1988) 1.
[37] M. B. Gavela, M. Lozano, J. Orloff and O. Pene, Nucl. Phys. B **430** (1994) 345; M. B. Gavela, P. Hernandez, J. Orloff, O. Pene and C. Quimbay, Nucl. Phys. B **430** (1994) 382; P. Huet and E. Sather, Phys. Rev. D **51** (1995) 379.
[38] M. Dine, P. Huet, R. L. Singleton, Jr and L. Susskind, Phys. Lett. B **257** (1991) 351; A. G. Cohen and A. E. Nelson, Phys. Lett. B **297** (1992) 111.
[39] P. Huet and A. E. Nelson, Phys. Rev. D **53** (1996) 4578; P. Huet and A. E. Nelson, Phys. Rev. D **53** (1996) 4578; M. S. Carena, M. Quiros, A. Riotto, I. Vilja and C. E. M. Wagner, Nucl. Phys. B **503** (1997) 387; J. M. Cline, M. Joyce and K. Kainulainen, Phys. Lett. B **417** (1998) 79 [Erratum-ibid. B **448** (1999) 321]; A. Riotto, Nucl. Phys. B **518** (1998) 339; A. Riotto, Phys. Rev. D **58** (1998) 095009; M. Trodden, Rev. Mod. Phys. **71** (1999) 1463; J. M. Cline and K. Kainulainen, Phys. Rev. Lett. **85** (2000) 5519; J. M. Cline, M. Joyce and K. Kainulainen, JHEP **0007** (2000) 018; M. S. Carena, J. M. Moreno, M. Quiros, M. Seco and C. E. M. Wagner, Nucl. Phys. B **599** (2001) 158; M. S. Carena, M. Quiros, M. Seco and C. E. M. Wagner, Nucl. Phys. B **650** (2003) 24.
[40] M. Carena, S. Heinemeyer, O. Stål, C. E. M. Wagner and G. Weiglein, Eur. Phys. J. C **73** (2013) 2552; S. Kanemura, H. Yokoya and Y. -J. Zheng, arXiv:1404.5835 [hep-ph]; B. Dumont, J. F. Gunion, Y. Jiang and S. Kraml, arXiv:1405.3584 [hep-ph].
[41] R. Barbieri, L. J. Hall and V. S. Rychkov, Phys. Rev. D **74** (2006) 015007; A. Goudelis, B. Herrmann and O. Stal, arXiv:1303.3010 [hep-ph]; Q. -H. Cao, E. Ma and G. Rajasekaran, Phys. Rev. D **76** (2007) 095011; E. Lundstrom, M. Gustafsson and J. Edsjo, Phys. Rev. D **79** (2009) 035013; E. Dolle, X. Miao, S. Su and B. Thomas, Phys. Rev. D **81** (2010) 035003 X. Miao, S. Su and B. Thomas, Phys. Rev. D **82** (2010) 035009; M. Gustafsson, S. Rydbeck, L. Lopez-Honorez and E. Lundstrom, Phys. Rev. D **86** (2012) 075019.
[42] M. Aoki, S. Kanemura and H. Yokoya, Phys. Lett. B **725** (2013) 302.
[43] A. M. Baldini, F. Cei, C. Cerri, S. Dussoni, L. Galli, M. Grassi, D. Nicolo and F. Raffaelli *et al.*, arXiv:1301.7225 [physics.ins-det].